

First-principles study of H on the reconstructed W(100) surface

K. Heinola and T. Ahlgren

Accelerator Laboratory, University of Helsinki, P.O. Box 43, Helsinki FIN-00014, Finland

(Received 6 November 2009; published 24 February 2010)

The first-principles calculations were used to study the hydrogen energetics on the (100) tungsten ($\sqrt{2} \times \sqrt{2}$)R45° surface. Two equilibrium sites for H at the surface are identified, with a low migration barrier from the energetically clearly higher long bridge site to the short bridge site. At low coverages, the majority of H surface diffusion events take place via the short bridge sites. The energetics for H penetration from the surface to the solute site in the bulk was defined, showing that the bulk H diffusion via neighboring tetrahedral sites takes place at depths beyond the second subsurface layer.

DOI: [10.1103/PhysRevB.81.073409](https://doi.org/10.1103/PhysRevB.81.073409)

PACS number(s): 71.15.Mb, 31.15.es, 66.30.je, 82.20.Db

Due to its extraordinary properties,¹ tungsten (W) is intended to be used as divertor plate material in the next step fusion device ITER.² Low-energy (1–100 eV) H isotopes escaping the plasma can congregate on the W surface or, when having high energies or high fluxes, penetrate through it and diffuse deeper into the bulk. In this Brief Report, detailed results for W(100) surface reconstruction and the energetics of low H coverage on this surface as obtained with calculations based on density functional theories (DFT), are presented. The H surface diffusivity has been deduced for the temperature range where the classical migration is predominant, i.e., the tunneling influence is negligibly small. In addition, the penetration energetics of H atom from the (100) surface to the bulk interstitial solute site is presented for the first time. Calculations of H diffusion in the bulk W are revisited and the results are presented at the end of this Brief Report. The results obtained in this study form the foundation of understanding the behavior of H on W surfaces.

The DFT calculations were performed with the Vienna Ab initio Simulation Package (VASP).^{3–5} Electronic ground state of the system was calculated using the projector-augmented wave^{6,7} potentials as provided in VASP. Electron exchange-correlation was performed within the generalized gradient approximation using Perdew-Burke-Ernzerhof functionals.^{8,9} Eight layers of W atoms separated by eight layers of vacuum were used for modeling of the surface properties. All atoms were allowed to relax. The used number of layers assured the bulklike properties in the middle of the W film. An H atom on the surface layer yields a surface coverage $\theta=0.03$, i.e., $\sim 6.2 \times 10^{13}$ H/cm². This corresponds to a saturated coverage of $\sim 19.9 \times 10^{14}$ H/cm², what agrees with the experimental result¹⁰ of $(19 \pm 2) \times 10^{14}$ H/cm². The migration barriers for hydrogen were calculated using the nudged elastic band (NEB) method.^{11,12}

The W(100) surface has been under thorough analysis both experimentally and computationally. Experiments have shown a complex temperature dependency of the reconstruction of the clean W(100) surface. At room temperature, the surface has $p(1 \times 1)$ periodicity,^{13,14} while at temperatures below a transition temperature $T_C \sim 250$ K the W(100) surface reconstructs to a lower energy level with $c(2 \times 2)$ structure.¹⁴ This reconstruction has a ($\sqrt{2} \times \sqrt{2}$)R45° unit cell and $p2mg$ symmetry, in which the surface layer atoms are laterally displaced to the $\langle 11 \rangle$ direction with a distance Δ from their ideal lattice positions. The displacement is originated by the bonding of the surface atoms with their nearest

neighbors located in the subsurface layer, forming a zigzag pattern on the surface advancing perpendicularly to the bonds with the subsurface atoms (see Fig. 1). The lateral surface displacement was found to be periodic with a wavelength of $\approx \sqrt{2}a$. The subsurface layers follow the surface reconstruction with decreasing Δ in order to release stresses induced by the top layer rearrangement.¹⁵ The DFT results up to four topmost layers are presented in Table I. The DFT calculations are in good agreement with the experimentally measured lateral displacements for the surface and the subsurface layer atoms of $\Delta_1=0.24$ Å and $\Delta_2=0.2 \cdot \Delta_1$, respectively.¹⁵ Moreover, the DFT results reveal the lateral displacement still occurring at the second subsurface with corresponding Δ_3 of $0.07 \cdot \Delta_1$. The interlayer distance between the surface and the first subsurface layer obtained with DFT (1.48 Å) agrees nicely with the experimental values reported by King and Thomas¹⁶ (1.48 Å) and by Altman *et al.*¹⁵

The transition temperature T_C increases almost linearly from 250 to 380 K with increasing H coverage θ from 0 to 0.3.²⁴ In addition, the surface symmetry changes from $\langle 11 \rangle$ to $\langle 10 \rangle$, i.e., from $p2mg$ to $c2mm$, at the coverage $\theta > 0.12$. The corresponding transition temperature for $\theta \approx 0.12$ is 306 K. In summary, the $c(2 \times 2)$ phase with $p2mg$ symmetry studied in this work occurs for the W surface with H coverages $0 \leq \theta < 0.12$.

Experiments have shown that H is adsorbed on the W(100) surface in the atomic form,²⁵ and that the adsorption site is the bridge site.²⁶ The DFT calculations performed in this study show that the H adsorption site on the W(100) surface turns out to be two different twofold bridge sites. For simplicity, they are called the short and the long bridge site. Figure 1 shows the H located at the short bridge site, which is 0.44 eV lower than the long one and therefore energetically more favorable. W–H bond length and W–H–W bond angle 2α were found to be 1.92 Å and $\approx 87.8^\circ$, respectively. The calculated 2α corresponds to a height above the surface, i.e., the distance of the equilibrium position of $d_{eq}=1.38$ Å. The adsorption energy of an H atom to a surface site was calculated as $E_{ads}=E_{WH}-(E_W+1/2E_{H_2})$, where E_{WH} is the total energy of a W–H system, E_W is the reference energy of the W(100) surface, and E_{H_2} is the energy of an H₂ molecule. Calculated values for E_{ads} are presented in Table II.

The experimental H vibration energies on $c(2 \times 2)$ surface with $\theta=0.01$ have been found to be $\nu_{SS} \approx 155$ meV,

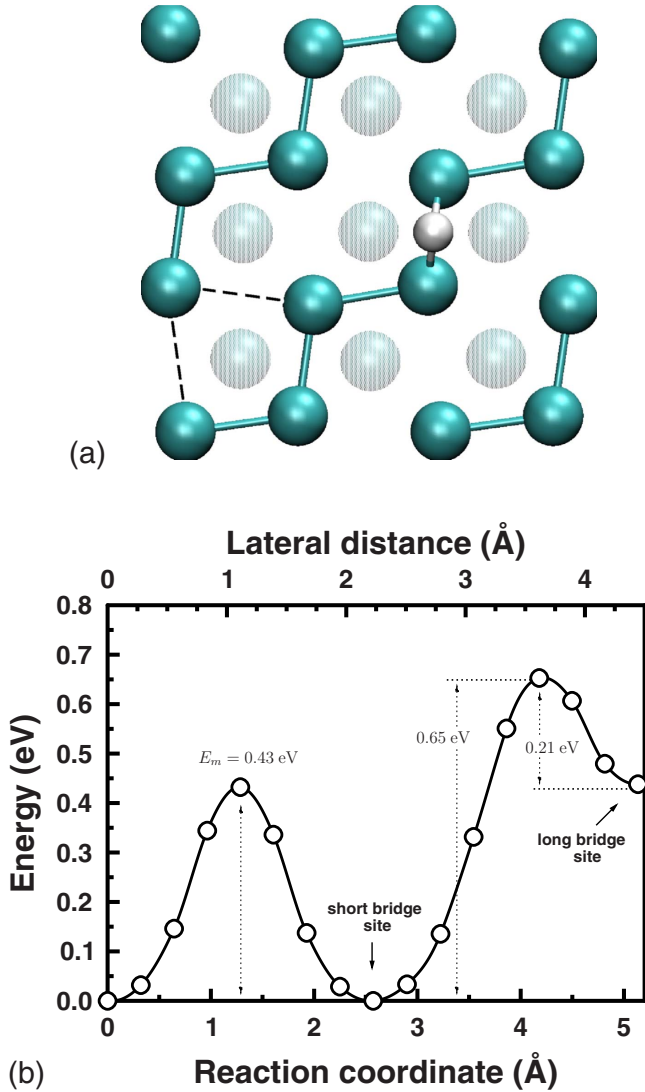


FIG. 1. (Color online) (a) Top view of the reconstructed W(100) surface with the H atom bonded to the twofold short bridge site. The dark and shaded spheres denote the surface and subsurface W atoms, respectively. The short bridge sites are marked as connection lines to the zigzag pattern. Two long bridge sites are highlighted with the dashed lines. (b) Potential energy pathway as a function of H position between adjacent short bridge sites and neighboring short bridge and long bridge sites using NEB.

$\nu_{AS} \approx 125$ meV, and $\nu_{wag} \approx 55$ meV.²⁶ Subscript indexes refer to the symmetric stretch (SS), asymmetric stretch (AS), and wag mode, respectively. For $\theta=0.03$, the ν_{AS} mode increases to ~ 130 meV, i.e., shifting toward ν_{SS} . Our results for the H vibration on the short bridge site were found to be $\nu_{SS}=163.5$ meV, $\nu_{AS}=138.1$ meV, and $\nu_{wag}=56.4$ meV, that agree well with the experiments. Corresponding vibration energies on the long bridge site are 130.3, 139.9, and 60.1 meV, respectively.

It has been shown experimentally that the pre-exponential factor and the activation energy for H diffusion on W(100) surface for $\theta=0.08$ and $220 \text{ K} < T < \text{RT}$ are $D_0=1.2 \times 10^{-2} \text{ cm}^2/\text{s}$ and $E_m=0.47$ eV, respectively.³² According to the results presented in this study, we identify that diffusion takes place along the short bridge sites, with DFT

TABLE I. Comparison of bulk and (100) surface properties of tungsten as obtained from experiment and DFT calculations: cohesive energy E_{coh} (eV/atom), lattice constant a (Å), surface energy σ (J/m²), atomic displacements Δ_i (Å) on the i^{th} layer and relative interlayer relaxation d_{ij} (%).

	Expt.	DFT	
		Other	Present work
bcc W			
E_{coh}	-8.89 ^a	-9.97, ^b -7.41 ^c	-8.48
a	3.165 ^a	3.14, ^b 3.22 ^c	3.172
W (100)			
σ	3.27, ^d 3.68 ^e	4.64 ^f	3.90
Δ_1	0.24 ^g	0.27, ^h 0.27 ⁱ	0.28
Δ_2	0.046 ^g	0.04, ^h 0.05 ⁱ	0.04
Δ_3		0.01, ^h 0.02 ⁱ	0.02
Δ_4		0.006 ⁱ	0.006
d_{12}	-4 ± 10 ^g	-7.8, ^h -6 ⁱ	-6.7
d_{23}		0.5, ^h 0.5 ⁱ	0.7
d_{34}		-0.5 ^h	-0.6

^aReference 1.

^bReference 17.

^cReference 18.

^dReference 19.

^eReference 20.

^fReference 21.

^gReference 15.

^hReference 22.

ⁱReference 23.

obtained values of $D_0=0.5 \times 10^{-2} \text{ cm}^2/\text{s}$ and $E_m=0.43$ eV, respectively. The diffusion path and the migration energy E_m between two adjacent ground states were calculated with the NEB method (Fig. 1). For finding the true energy path minimum between two ground states, the NEB calculations are performed allowing all atoms to relax. Since the diffusing H atom has a high vibrational frequency compared to the surrounding W atoms, it is questionable whether the W atoms are mobile in time scales of the H overbarrier motion. Therefore, the migration barrier between adjacent short bridge sites was recalculated, allowing no relaxation for the W atoms during the H overbarrier motion, resulting in $E_m=0.45$ eV, which is in even better agreement with the experimental value.

The D_0 was obtained by calculating the vibrational frequencies on the saddle point and on the ground state using the concept of classical harmonic transition state theory (TST).^{33,34} The tunneling crossover temperature, T_x , under which the nonclassical migration becomes dominant, was evaluated using the tunneling model by Fermann and Auerbach.³⁵ The model gives $T_x \sim 138$ K, proving that our calculations with classical TST are valid at the temperature range used in the experiments.

A schematic energy landscape for H in the vicinity of the surface and in the lattice interior as a function of depth is presented in Fig. 2. An adsorbed particle must overcome the energy barrier of E_{s2b} in order to be located in a lattice site with energy S' . The calculated energetics for H penetration from the short bridge site to the interstitial solute site in the

TABLE II. Properties of the H in bulk W and on reconstructed W(100) surface as obtained from experiment and DFT calculations: enthalpy of solution S (eV), energy difference of octahedral (O) and tetrahedral (T) solution sites ΔE_{O-T} (eV), pre-exponential factor for bulk diffusion D_0 (m^2/s), the adsorption energy E_{ads} (eV/H), and the migration energy E_m (eV) of the relaxed (unrelaxed) overbarrier motion in the bulk and on various surface sites.

	Expt.	DFT		
		Other	Present work	
H solution				
S	1.04 ^a		0.95	
ΔE_{O-T}		0.38 ^b	0.38	
E_m	0.39 ^a	0.20 ^c	0.21 (0.26)	
D_0	4.1×10^{-7} ^a		5.2×10^{-8} (4.8×10^{-8})	
	Expt.	Present work		
H on W (100)				
	E_{ads}	E_m	E_{ads}	E_m
Short bridge	0.7, ^d 0.82 ^e	0.47 ^f	0.91	0.43 (0.45)
Long bridge			0.47	0.43 (0.48)
Short \curvearrowright Long				0.65 (0.67)
Short \curvearrowleft Long				0.21 (0.24)
E_{s2b}				2.03
E_{b2s}				0.27

^aReference 27. Experimental data 1100 K $< T < 2500$ K. Arrhenius fit to the data points over 1500 K yields $D_0 = 1.58 \times 10^{-7}$ m^2/s and $E_m = 0.25$ eV.

^bReferences 28 and 29.

^cReference 30.

^dReferences 31 and 16.

^eReference 10.

^fReference 32.

bulk is presented in Fig. 3. The probability of an H atom moving from the surface to the bulk is very small since the potential barrier is found to be ~ 2 eV. On the other hand, in the absence of deep traps in the bulk, the H atoms are easily accumulated from the bulk to the surface since the migration barriers to the surface, E_{b2s} , and in the bulk, E_m , are almost identical (Table II).

The H solution energy for the eight layer W film used in this study was found to be $S' = 0.84$ eV, which is somewhat lower than the value calculated for the bulk S (Table II).³⁶ As an additional verification to our calculations, the summation of absolute values of E_{ads} and S' (according to the model shown in Fig. 2), should result in the same value for the solute site energy with respect to the surface site as obtained in the NEB calculations. And indeed this is the case, since $E_{\text{ads}} + S' = E_{s2b} - E_{b2s}$ holds (see Table II and Fig. 2 for the definitions).

In our previous DFT study on H diffusion in bulk W,³⁶ it was found that the bulk migration barrier E_m , and the diffusion pre-exponential factor D_0 , agree with the experimental values in the temperature range 1500 K $< T < 2400$ K, where no H trapping defects are present.^{37,38} An Arrhenius fit to the experimental data points in that temperature region

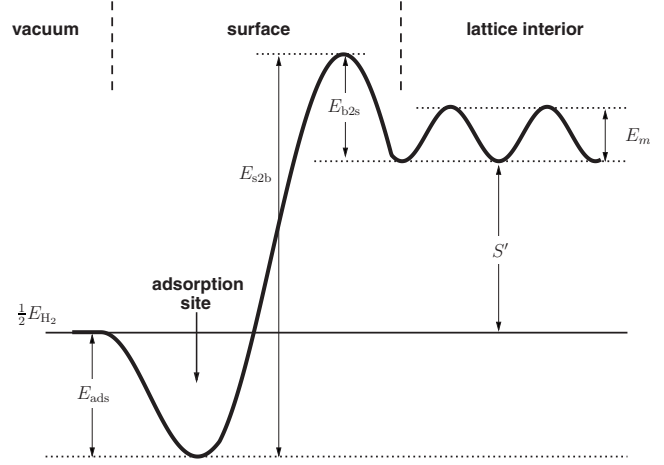


FIG. 2. Schematic one-dimensional energy landscape of a solid, which absorbs H endothermally. In the vacuum (left side), the H is in molecular form with energy E_{H_2} , while atomic H is adsorbed on the surface with the adsorption energy E_{ads} . Here, it is supposed that the atomic desorption energy equals to the adsorption energy, $E_{\text{des}} \approx E_{\text{ads}}$. The H atom must overcome the energy barrier of E_{s2b} in order to penetrate through the surface to a solute site with energy S' . The reversible motion from solute site to the surface requires energy of E_{b2s} . E_m is the bulk diffusion barrier.

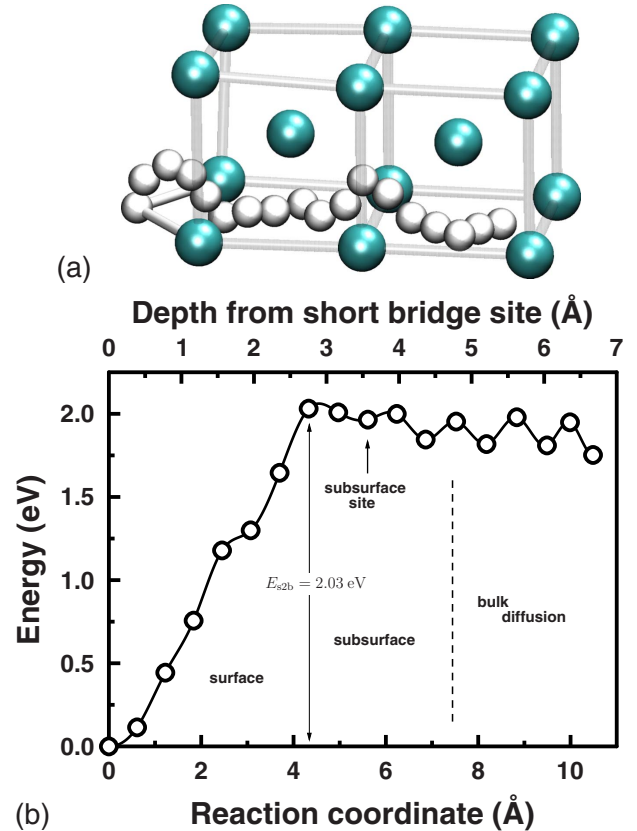


FIG. 3. (Color online) (a) Migration path of H absorption from surface short bridge site to the solute site in the lattice interior as obtained with NEB. After the second subsurface layer, the migration proceeds via neighboring tetrahedral sites. (b) NEB result for the energetics of H absorption. A local ground state in the subsurface region can be identified as the subsurface site.

resulted in $E_m=0.25$ eV and $D_0=1.6 \times 10^{-7}$ m²/s, that were in good agreement with the DFT results³⁶ (0.21 eV and 5.2×10^{-8} m²/s, respectively). Utilization of the NEB calculation with unrelaxed W atoms along the diffusion path results in $E_m=0.26$ eV and $D_0=4.8 \times 10^{-8}$ m²/s. The D_0 is found in good and the E_m in perfect agreement with the fit to the experimental data points over 1500 K.

To summarize, the energetics of atomic H on W(100) surface with low coverages and temperatures \leq RT has been investigated utilizing the DFT calculations. Two bridge sites for adsorption were identified. Due to their difference in energetics, the lower bridge site is concluded to be the dominant adsorption site: the diffusion of H on W(100) surface proceeds via neighboring short bridge sites at low temperatures and coverages. The surface diffusion barrier between two adjacent short bridge sites was calculated with the NEB method and the jump rate was deduced according to the TST.

The resulting diffusion parameters showed good agreement with the experimental data. The energetics of the hydrogen penetration into solute site of bulk W has been presented. The potential barrier for the surface to bulk migration was found to be relatively large, whereas the barrier for reversible motion was found to be virtually as high as the migration barrier for the diffusion in the bulk. The H diffusion parameters in bulk W has been recalculated using unrelaxed W atoms, giving perfect agreement for the diffusion barrier compared to the experimental data above 1500 K.

This work, supported by the European Communities under the contract of Association between Euratom-Tekes, was carried out within the framework of the European Fusion Development Agreement (EFDA). Grants of computer time from the Center for Scientific Computing (CSC) in Espoo, Finland are gratefully acknowledged.

-
- ¹E. Lassner and W.-D. Schubert, *Tungsten—Properties, Chemistry, Technology of the Element, Alloys, and Chemical Compounds* (Kluwer Academic, New York, 1999).
- ²A. Loarte *et al.*, Nucl. Fusion **47**, S203 (2007) and references therein.
- ³G. Kresse and J. Hafner, Phys. Rev. B **47**, 558 (1993).
- ⁴G. Kresse and J. Hafner, Phys. Rev. B **49**, 14251 (1994).
- ⁵G. Kresse and J. Furthmüller, Phys. Rev. B **54**, 11169 (1996).
- ⁶P. E. Blöchl, Phys. Rev. B **50**, 17953 (1994).
- ⁷G. Kresse and D. Joubert, Phys. Rev. B **59**, 1758 (1999).
- ⁸J. P. Perdew, K. Burke, and M. Ernzerhof, Phys. Rev. Lett. **77**, 3865 (1996).
- ⁹Y. Zhang and W. Yang, Phys. Rev. Lett. **80**, 890 (1998).
- ¹⁰P. Alnot, A. Cassuto, and D. A. King, Surf. Sci. **215**, 29 (1989).
- ¹¹G. Mills, H. Jonsson, and G. K. Schenter, Surf. Sci. **324**, 305 (1995).
- ¹²H. Jonsson, G. Mills, and K. W. Jacobsen, *Classical and Quantum Dynamics in Condensed Phase Simulations* (World Scientific, Singapore, 1998).
- ¹³T. E. Felter, R. A. Barker, and P. J. Estrup, Phys. Rev. Lett. **38**, 1138 (1977).
- ¹⁴M. K. Debe and D. A. King, Phys. Rev. Lett. **39**, 708 (1977).
- ¹⁵M. S. Altman, P. J. Estrup, and I. K. Robinson, Phys. Rev. B **38**, 5211 (1988).
- ¹⁶D. A. King and G. Thomas, Surf. Sci. **92**, 201 (1980).
- ¹⁷T. Ochs, O. Beck, C. Elsasser, and B. Meyer, Philos. Mag. A **80**, 351 (2000).
- ¹⁸N. Juslin, P. Erhart, P. Träskelin, J. Nord, K. O. E. Henriksson, K. Nordlund, E. Salonen, and K. Albe, J. Appl. Phys. **98**, 123520 (2005).
- ¹⁹W. R. Tyson and W. A. Miller, Surf. Sci. **62**, 267 (1977).
- ²⁰F. R. de Boer, R. Boom, W. C. M. Mattens, A. R. Miedema, and A. K. Niessen, *Cohesion in Metals* (North-Holland, Amsterdam, 1988).
- ²¹L. Vitos, A. V. Ruban, H. L. Skriver, and J. Kollar, Surf. Sci. **411**, 186 (1998).
- ²²D. Spišák and J. Hafner, Phys. Rev. B **70**, 195426 (2004).
- ²³R. Yu, H. Krakauer, and D. Singh, Phys. Rev. B **45**, 8671 (1992).
- ²⁴R. A. Barker and P. J. Estrup, J. Chem. Phys. **74**, 1442 (1981).
- ²⁵A. Adnot and J. D. Carette, Phys. Rev. Lett. **39**, 209 (1977).
- ²⁶M. R. Barnes and R. F. Willis, Phys. Rev. Lett. **41**, 1729 (1978).
- ²⁷R. Frauenfelder, J. Vac. Sci. Technol. **6**, 388 (1969).
- ²⁸K. O. E. Henriksson, K. Nordlund, A. Krasheninnikov, and J. Keinonen, Fusion Sci. Technol. **50**, 43 (2006).
- ²⁹C. Becquart and C. Domain, J. Nucl. Mater. **386-388**, 109 (2009).
- ³⁰Y.-L. Liu, Y. Zhang, H.-B. Zhou, G.-H. Lu, F. Liu, and G.-N. Luo, Phys. Rev. B **79**, 172103 (2009).
- ³¹P. W. Tamm and L. D. Schmidt, J. Chem. Phys. **51**, 5352 (1969).
- ³²L. Cai, M. S. Altman, E. Granato, T. Ala-Nissilä, S. C. Ying, and X. Xiao, Phys. Rev. Lett. **88**, 226105 (2002).
- ³³E. Wigner, Z. Phys. Chem. Abt. B **19**, 203 (1932).
- ³⁴H. Eyring, J. Chem. Phys. **3**, 107 (1935).
- ³⁵J. T. Fermann and S. Auerbach, J. Chem. Phys. **112**, 6787 (2000).
- ³⁶K. Heinola and T. Ahlgren, J. Appl. Phys. (to be published).
- ³⁷E. Serra, G. Benamati, and O. V. Ogorodnikova, J. Nucl. Mater. **255**, 105 (1998).
- ³⁸G. Benamati, E. Serra, and C. H. Wu, J. Nucl. Mater. **283-287**, 1033 (2000).